Annu. Rev. Phys. Chem. 1995. 46: 197–222

DYNAMICS AND PHOTOCHEMISTRY OF NEUTRAL VAN DER WAALS CLUSTERS

Elliot R. Bernstein

Department of Chemistry, Colorado State University, Fort Collins, Colorado 80523

KEY WORDS: electron transfer, intermolecular vibrational redistribution, proton transfer, radical addition cluster chemistry, vibrational predissociation

ABSTRACT

This review covers the field of excited electronic-state chemical reactions in small clusters. The clusters emphasized are those comprised of an organic chromophore that is electronically excited to initiate the reaction and of various coreactant molecules ranging from water and ammonia to ethers, amines, aromatics, alkanes, alkenes, and diatomics. The reactions discussed include vibrational relaxation, vibrational predissociation, electron transfer, proton transfer, and radical additions. The reactions are analyzed based on laser-induced fluorescence excitation, dispersed emission, mass-resolved excitation spectroscopy, stimulated emission pumping, and picosecond time-resolved implementation of these spectroscopies.

INTRODUCTION

In the last 15 years, the study of chemical dynamics (among other areas) has been greatly advanced by three experimental developments: time-resolved (nanosecond, picosecond, femtosecond) laser techniques, supersonic expansion sample preparation, and generation of homogeneous and heterogeneous clusters of neutral species. This review mainly focuses on the use of time-resolved optical methods applied to van der Waals clusters, generated in a supersonic expansion, to elucidate elementary processes in

0066-426X/95/1101-0197$05.00

energy dynamics and photochemistry of simple, well-controlled molecular systems. In some instances, only spectroscopic studies have been employed to study the photochemistry of clusters, and these cases are also reviewed because they serve well to elucidate elementary photochemical processes. In this discussion we closely examine four separate but interrelated topics of intermolecular processes: (*a*) intracluster vibrational energy redistribution (IVR) and cluster vibrational predissociation (VP), (*b*) intracluster electron transfer

$$(DA \xrightarrow{h\nu} D^*A \quad \text{or} \quad DA^* \rightarrow D^+A^-),$$

(*c*) intracluster proton transfer

$$[ROH(X)_n \xrightarrow{h\nu} R^*OH(X_n) \rightarrow R^*O^- \cdots H^+(X_n)],$$

and (*d*) intracluster reaction of excited-state reactive intermediates (e.g. radicals, carbenes, nitrenes) with neutral molecular species.

These dynamical events all have an essential feature in common: They are all initiated by the absorption of a photon that excites a chromophore molecule in the cluster from the singlet S_0 or doublet D_0 ground state to an excited electronic state. This event occurs at the instigation of the experimenter and serves as the system timing pulse for the measurement of the ensuing dynamical processes. Vibrational dynamics on the ground electronic-state surface can also be followed by population of vibrational modes through emission (1–8), stimulated emission pumping (SEP) (9–13), Raman pumping (14–17), or direct infrared absorption (18).

Clusters are an essential component of the fundamental study of intermolecular interactions and structures, energy dynamics, and photochemistry. Because they are formed and cooled in a supersonic expansion, clusters are accessed at a known energy and geometry and are effectively isolated from collisions and further interactions (19–21). Although not all clusters are rigid [e.g. $C_6H_6(N_2)_1$ in which the N_2 center of mass lies on the sixfold ring axis of benzene and the N_2 bond axis is perpendicular to it] (22–25), at least they are in low-lying energy states characterized by low-temperature thermal transitional, rotational, and vibrational distributions. Because clusters can be size-selected (see below) or size-detected (19) and can often be identified with respect to a particular structure (isomer) for a given size (26–30), one can evaluate the relation between size, structure, energy levels, and dynamics and reactivity in a cluster system. Because of these properties, clusters are one of the few systems for which detailed ab initio theory of bimolecular processes and solvation can presently be calibrated (25, 31–39). Clusters thus play a central role in the current effort to unravel many of the collective properties (structure, energy levels,

internal motion, solvation) and phenomena (e.g. chemical reactions, dynamics, redistribution of energy, coherence) addressed by modern physical chemistry research.

The study of dynamics and chemistry in van der Waals clusters has not only grown too large to be reviewed usefully in the space allotted for this chapter, but has become too far ranging to be critically reviewed by a single reviewer with a particular set of experiences, interests, and a limited area of expertise. Before we narrow the focus of this review and begin discussion of excited electronic-state van der Waals complex vibrational dynamics, electron transfer and proton transfer reactions, and radical reactions, a short historical introduction of this general area is perhaps useful. Although one is always on thin ice when claiming a particular group was first in a given area, the efforts of a few groups are worth mentioning because they seem to have had pivotal roles in the early stages of this field. The time-resolved dynamical studies of Rettschnik and coworkers (40–44) on tetrazine-Ar clusters first led us to suggest that IVR-VP processes are serially related and that they obey statistical unimolecular reaction rate theory (45). Early studies of chemical reactions in clusters come from the groups of Jouvet & Solgadi (46) and Wittig and coworkers (47–49). Jouvet & Solgadi (46) studied electronically excited metal atoms (Hg) clustered with potential reactants (H_2). Wittig and coworkers (47–49) investigated hot-atom

$$(HX \xrightarrow{h\nu} H + X)$$

reactions in ground electronic-state clusters

$$(\text{e.g. } XHCO_2 \xrightarrow{h\nu} X + H \cdots OCO \rightarrow OH + CO).$$

Both of these studies have been reviewed many times and most recently in a review book (47). An interesting and important variation on these themes comes from the work of Neumark and coworkers (50, 51), which involves the photodetachment of an electron from a stable nonreactive anion to initiate a reaction.

One of the more important aspects of cluster studies is the identification of the mass of the clusters accessed by photoexcitation and prepared in a nonequilibrium state from which relaxation or reaction can occur. As long as the excitation, reaction, dynamics, and/or photoionization processes do not cause cluster fragmentation, the identification of a cluster is typically straightforward to within ± 1 amu. If fragmentation takes place, the cluster mass information is typically lost, with a concomitant loss of important physical information. We begin this review by discussing three techniques

that can be employed (with some success in many instances) to overcome those difficulties.

Following this latter discussion, we cover the cluster phenomena alluded to above: IVR-VP, electron transfer, proton transfer, and radical reactions.

MASS SELECTION AND DETECTION OF NEUTRAL CLUSTERS

Spectroscopy and photochemistry of ionic clusters are aided by the ready availability of mass resolution of both reactant and product species. A charged cluster can be put through a stage of mass filtering and/or selection such that a beam of single-mass species can be generated and accessed. In such a regime, one then knows that cluster fragmentation from higher-mass species does not confuse the experimental intensity or energy distribution of products. Thus, for example, the $AX_n^+ \rightarrow AX_{n-2}^+ + X_2$ reaction can be singled out for study without interference from contributions to the AX_n^+ and AX_{n-2}^+ mass channels from cluster ions of other masses. In general this is not so for neutrals, however, because a typical neutral beam consists of clusters of a number of different masses that can fragment upon excitation

$$(\text{e.g. } AX_n \xrightarrow{h\nu} A^*X_n \rightarrow A^*X_m + X_{n-m})$$

and/or ionization

$$(\text{e.g. } A^*X_n \xrightarrow{h\nu} AX_n^+ \rightarrow AX_m^+ + X_{n-m}).$$

Thus, mass selection for neutral beams is a valuable goal.

One rather impractical method of mass selection of neutrals is to ionize them, mass select them, and then neutralize them; one has no guarantee that the neutralization process will not cause fragmentation. A more useful approach has been taken by Buck (52). The technique involves forming clusters in a (pulsed) supersonic expansion that is subsequently crossed by another (pulsed) supersonic expansion consisting of pure expansion gas (He or other inert or rare gas). The atoms, molecules, and clusters in the two intersecting expansions collide and transfer momentum, and the clusters are scattered out of the first expansion beam at an angle proportional to their mass or size. Thus, clusters of different mass are spatially separated in the apparatus. A movable mass detector is useful in this instance. This process of mass selection has two disadvantages: It can cause vibrational and rotational (internal and external) excitation in the cluster, and each mass-selected species will typically be of low concen-

tration. Nevertheless, the method has found a considerable degree of application.

A second method of parent mass identification of clusters, even in the face of extensive neutral or ionic fragmentation, arises owing to the nature of a pulsed expansion and its dynamics (53–56). Two events occur in a pulsed nozzle supersonic expansion that allow mass determination to be made for the clusters. First, the time needed to form clusters is longer for larger clusters than smaller ones. Second, some velocity slip occurs for species of different masses: He travels fastest, the dopant monomers are the next fastest species, the one-to-one clusters are the next fastest, and so on. The arrival distribution time of species with different masses is maximum at different places (times) in the gas pulse with respect to the nozzle trigger pulse. Thus, spectroscopic features appearing in a given mass channel (timed by the ionization pulse) will have different intensity profiles with regard to the nozzle triggering pulse. These peak differences can be ~ 10 μs per 20 amu for clusters ~ 100–200 amu in a time-of-flight mass spectrometer. This arrival time difference allows one to identify the cluster mass parentage of different spectroscopic features measured in a given mass channel. Cluster spectra observed by monitoring a particular mass channel will have timing (arrival time) distributions with respect to the nozzle timing pulse that are characteristic of their parent cluster flight time from the nozzle to the mass spectrometer ionization region. At higher cluster masses, however, these arrival time differences become smaller, and the intensity differences become more difficult to discern.

A very recent and elegant third method of mass identification of neutral species in a beam has been demonstrated by Toennies and coworkers (57). This mass separation method relies on the wave nature of particles in a cold beam. An interference pattern is generated following transmission of the beam through a diffraction grating. The diffraction pattern thus created depends on the mass and velocity ($\lambda = h/mv$) of the particles in the beam and on the diffraction law $n\lambda = 2d \sin \theta$. For $(H_2)_n$, $(He)_n$, the angles of diffraction are ~ 1 mrad or less. At present, this approach does not appear to be applicable to larger or heavier systems, but one should note that it is quite new and depends heavily on state-of-the-art machining technology, which is presumably rapidly advancing.

CLUSTER DYNAMICS—INTRACLUSTER VIBRATIONAL ENERGY REDISTRIBUTION AND CLUSTER VIBRATIONAL PREDISSOCIATION

The separate and distinct processes of IVR and cluster VP are closely related to the more general phenomena of radiationless transitions (58–

60) (e.g. internal conversion and intersystem crossing) and unimolecular reaction rate theory (61–64) (e.g. RRKM theory). As such, two concepts in particular play central roles in the understanding of these cluster processes: density of vibrational states (especially low-energy molecular and intermolecular modes) and the nature of the coupling matrix elements between the initial (prepared) states and the final (relaxed) states. Systems are classified in these theories according to their density of states: small, intermediate, and large. In the small-system limit, the density of states is low (e.g. <0.1 per cm^{-1}) and the matrix elements control the dynamics. This is the case for $I_2(He)_1$ clusters (65), for which IVR and VP are slow and occur simultaneously in a process described as

$$I_2(v' = 22)\,He \rightarrow I_2(v' = 21) + He.$$

Neither Fermi's Golden Rule nor RRKM theory can be used to describe such behavior, which is best dealt with as a direct coupling between the bound and continuum states (66, 67). In an intermediate density-of-states system (e.g. ~ 1 to 10 per cm^{-1}), one could observe nonexponential decay (beats) behavior, with some excitation energies showing the small-system limit and others not. This type of behavior could be observed at low vibrational excitation for polyatomic clusters such as $SO(N_2)_1$ or perhaps even $I_2(N_2)$. To the best of our knowledge, no such experimental elucidation of this behavior for clusters has been demonstrated to date. The large-system limit has a density of vibrational states greater than 10 to 100 per cm^{-1} and exponential decays. RRKM or statistical theories apply here, and no beat phenomena are observed. This latter case is found for aniline (68–70), indole (71, 72), perylene (73, 74), and tetrazines (40–44) clustered with rare gases, and diatomic and polyatomic molecules. When the density of internal cluster states is high, the coupling to them dominates the small coupling to the free-particle continuum states, and IVR precedes VP. One can readily demonstrate this by cluster vibronic excitation, which is energetically insufficient to break the cluster van der Waals bond but large enough to encounter a sufficient density of cluster states to facilitate IVR within the excited electronic state lifetime. All of the above systems are shown to behave in this manner. In particular, for rare gas solvents such as Ar, the van der Waals vibrational space is small enough (only three modes) such that the VP is very fast (<10 ps), but the cluster decay, $[C_6H_5NH_2(Ar)_1]^* \rightarrow C_6H_5NH_2 + Ar$, is quite slow because of the IVR (~ 5 ns) bottleneck (45). In this reaction the aniline remains electronically excited but not vibrationally excited; the vibrational energy (~ 500 to 800 cm^{-1}) goes into van der Waals bond breaking and translational (and perhaps rotational) energy of the products. This work has been reviewed recently (75). It was initiated by the early time-resolved results of Retts-

chink and colleagues (40–44) on tetrazine$(Ar)_1$ and the subsequent studies of Kelley, Bernstein, and coworkers (45, 68, 69). A number of groups have now shown that for high density-of-states systems (e.g. atomic, diatomic, or polyatomic solvation of a polyatomic chromophore), IVR and VP are related in a serial fashion (first IVR from the accessed chromophore modes to cluster van der Waals modes occurs, and then VP can occur), that both are statistical, and that Fermi's Golden Rule and RRKM theory of unimolecular reactions are the applicable first-order approaches for modeling these cluster vibrational dynamics (40–44, 68–74).

These conclusions depend not so much on the details of the numerical results for the decay times, but on their qualitative trends and nature. First, IVR itself can be seen to be fast or slow from the initial vibronic state accessed if the vibrational energy in the cluster is not sufficient to break the cluster van der Waals bond. If this decay time, τ_{IVR}, is known at a given vibrational energy, it can be predicted with some confidence at other energies. Second, if τ_{VP} is very fast (<10 ps), many intermediate states for the IVR process will dissociate and the bare molecule will be left in the vibronically excited states appropriate for energy conservation. This too is observed if the van der Waals space is small [e.g. aniline$(Ar)_1$] and if the appearance time for the bare molecule equals τ_{IVR}. Third, if IVR is very fast and VP is slow [e.g. aniline$(CH_4)_1$], only the lowest level of the cluster or bare molecule excited electronic state will be populated during the total IVR-VP process, and the disappearance time of the cluster and the appearance time of the bare molecule will be nearly equal to τ_{VP}. Finally, in the intermediate case [e.g. aniline$(N_2)_1$], the population of intermediate states of the cluster and the appearance of bare molecule states do not have time constants equal to either τ_{IVR} or τ_{VP}. The decay and rise times of these signals are related to τ_{IVR} or τ_{VP} in a more complex manner, as given by standard consecutive first-order rate processes (76). All of this qualitative behavior is by now well documented for the systems studied in detail (75).

These ideas still leave room for special modes and special couplings if the matrix elements that appear in Fermi's Golden Rule and statistical reaction rate theories can vary for different states accessed by laser excitation. One can evaluate the importance of various modes for the relaxation processes in and dissociation of clusters by changing the composition of the active or important vibrational space. A good example of this approach is found in the IVR-VP studies of 4-ethylaniline by Hineman et al (69). In this instance, the ethyl tail on the aniline chromophore presents two important additional low-energy modes that can potentially add to the van der Waals space: a bending mode at $\sim 84(100)$ cm^{-1} for $S_1(S_0)$ and a $35(47)$ cm^{-1} torsional mode. Both of these modes, because they are low

in energy, could effectively add to the overall density of states of the clusters, thereby enhancing the IVR decay rates and reducing the VP rates. These modes change the VP rates not only by adding to the density of states, but also by removing energy from the VP-active van der Waals modes.

Two situations can arise from clusters involving such species. First, τ_{IVR} can be slow and τ_{VP} can be fast [e.g. 4-ethylaniline$(Ar)_1$]. In this instance, the excited vibrational state of the chromophore decays into the high density of states of the cluster, but VP occurs as soon as the van der Waals modes have sufficient energy. The chromophore is then left with a distribution of 35(47) and 84(100) cm^{-1} mode intensity in its emission that resembles a Franck-Condon envelope of transition probabilities. This shows that 35 and 84 cm^{-1} modes are populated, not specially, but as they contribute to the overall clusters density of states at a given vibronic energy of excitation. Second, τ_{IVR} can be fast and τ_{VP} can be slow [e.g. 4-ethylaniline$(N_2$ or $CH)_1$]. In this case, vibrational energy in the cluster has a chance to equilibrate, and the cluster develops a vibrational temperature (equilibrium) prior to the VP process. The emission from the bare chromophore then displays a sequence progression in the 35(47) cm^{-1} torsional mode (a group of 12 cm^{-1} spaced bands about the 0_0^0 transition) that reflects a Boltzmann intensity distribution. Although the torsional mode appears to be special, it only arises because it is low in energy and in equilibrium with the other low-energy modes in the van der Waals vibrational space.

This IVR-VP behavior is completely statistical in both cases given above and allows one to make a final product state determination for the overall dynamics and reaction that occur in these chromophore-solvent clusters. The central determining factor for the vibrational dynamics of these clusters is the total (van der Waals plus chromophore) density of low energy modes.

PHOTOINDUCED ELECTRON TRANSFER REACTIONS

Electron transfer reactions have been studied in small clusters for several different systems and in several different physical situations. A good review of the early work in this area can be found in Reference 77. In this section we first discuss some of the general ideas behind electron transfer in van der Waals complexes and some specially designed donor and acceptor single-molecule systems. In particular we define excimer, exciplex, charge-transfer complex, and oxidative and reductive electron transfer, and discuss limiting interactions, states, energies, and potential energy surfaces

for the process of interest. Following these preliminaries we review a few different types of electron transfer or charge-transfer systems.

Some Definitions and Preliminaries

A *van der Waals complex* is a collection of two or more atoms or molecules held together by van der Waals or dispersion forces in both ground and excited electronic states. The typical van der Waals systems could be modeled by a Lennard-Jones, exponential-six, Morse or other potential form that gives a good representation of dispersion interactions (75). In a supersonic expansion such molecular clusters are readily formed and have binding energies between ~ 500 and 1500 cm^{-1} (e.g. C_6H_6/CH_4, NH_3, H_2O). In solution or in the gas phase at 300 K, one would consider these clusters to be unbound.

An *excimer* is a van der Waals complex of identical atoms or molecules that has a much more strongly bound excited state than ground state. The increased excited-state interaction arises from a resonance exchange or exciton interaction in the excited state. This can be expressed as

$$MM \xrightarrow{h\nu} M^*M \rightarrow [M^*M \pm MM^*]$$

in which MM represents a ground-state van der Waals complex (probably unbound at 300 K), and M^*M and MM^* represent localized excited-state clusters. The linear combination of local excited states through the exchange or exciton interaction occurs over and above the usual ground- or excited-state dispersion interactions. The additional excited-state interaction can be quite strong ($\sim 10^4$ cm^{-1}) and can lead to a completely different physical system than a van der Waals cluster.

An *exciplex* is a more complicated system: It consists of two or more unlike molecules. The ground state of this complex is still a van der Waals system, at least to first order. The excited state of this type of cluster is, however, different from that of an excimer. The exciton interaction for a complex of different molecules is greatly damped due to the absence of resonance exchange. The interaction that now dominates the excited state is electron transfer, which depends on the ionization potential (IP) of the donor (D) partner and the electron affinity (EA) of the acceptor (A). At the equilibrium geometry of the excited exciplex, the ground state of the cluster is dissociative.

The schematic representation of an exciplex system is given as

$$DA \xrightarrow{h\nu} D^*A \rightarrow D^+A^-$$

or

$$DA \xrightarrow{h\nu} DA^* \rightarrow D^+A^-.$$

In a supersonic jet cluster environment, the DA ground-state cluster is bound by a comparatively weak van der Waals interaction, and the binding energy of the charge-transfer state D^+A- is quite large and proportional to the Coulomb interaction of the separated charges. The charge or electron transfer transition appears at an approximate energy of

$$\Delta E_{CT} \sim (IP)_D - (EA)_A - e^2/R + \ldots$$

A somewhat more quantitative discussion of these points can be found in the review by Haas & Anner (77).

The electronic potential energy surfaces for such an exciplex system can be represented schematically as shown in Figure 1. Excitation from the ground electronic state of the cluster to the excited state typically occurs through the van der Waals excited state, owing to Franck-Condon and symmetry considerations. Population of the CT (or ET) state occurs as a relaxation or radiationless transition. The two excited-state potential surfaces can undergo a crossing or an avoided crossing depending on the details of the complex symmetry and on the crossing point. If a barrier develops at the avoided crossing, the kinetics of the radiationless process can be measured. In some instances the ET state can be directly accessed in the optical transition. The wave functions for all three electronic states illustrated in Figure 1 can be expressed as

$$\Phi_i = a^i\Psi(DA) + b^i\Psi(D^+A^-) + c^i\Psi(D^*A \text{ or } DA^*),$$

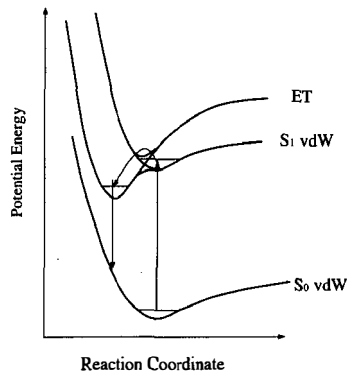

Figure 1 Potential energy surfaces for an electron transfer cluster. Arrows indicate adsorption, relaxation and emission. Note that at the ET-state equilibrium position, the cluster is dissociative on the ground-state (S_0) surface.

in which Φ_i represents the ith electronic state wave function; i represents the ground, vdW excited, or ET states; a, b, and c are mixing coefficients, as indicated; and $\Psi(MN)$ represents the appropriate zeroth-order wave function for the indicated limiting model state. Direct optical transitions to the excited ET state from the ground state are typically weak if the cluster ground state is mostly of a van der Waals nature ($a \sim 1$).

A *charge transfer* complex is said to occur if the b^g coefficient in the cluster Φ_g becomes large ($b^g \sim 1$) so that charge separation occurs in the unexcited cluster. With regard to Figure 1, the lowest ET state (potential energy surface) would fall below the energy of the ground-state van der Waals potential energy surface.

Within the context of the exciplex and electron transfer systems, two types of excited-state electron transfer reactions can be photoinduced. Consider first the situation in which the electron acceptor is excited:

$$DA \xrightarrow{h\nu} DA^* \rightarrow D^+A^-.$$

In this instance the donor contributes an electron to the acceptor from its highest occupied molecular orbital, that is, the donor filled orbitals are higher in energy than the acceptor filled orbitals. This electron transfer is referred to as reductive quenching of the photoexcited acceptor. Anthracene and aniline systems fall into this category. The second type of exciplex electron transfer comes about by photoexcitation of the donor:

$$DA \xrightarrow{h\nu} D^*A \rightarrow D^+A^-.$$

In this instance the donor excited electron experiences a reduced IP because the optical transition has added some 4 to 6 eV to the donor energy. This is typically referred to as oxidative quenching of the photoexcited donor. In either of these two instances, oxidative or reductive quenching, the cluster may emit from the excited ET state to the repulsive (see Figure 1) ground-state surface, and the equilibrium relationship between IP, EA, and the Coulomb interaction for the overall charge or electron transfer process must hold.

Reductive Electron Transfer: $DA^* \rightarrow D^+A^-$

The review by Haas & Anner (77) of work published prior to 1988 is an excellent source of reference to the early efforts in this area. The general form of these studies is to employ a polycyclic aromatic moiety as an acceptor molecule to be excited and an aniline, amine, or ether species as the donor. The groups of Levy (78–80), Lim (81–85), Tramer (86, 87), Haas (77, 88, 89), and Rettschnick (90, 91) have made significant recent experimental contributions to this field, while Jortner et al (92, 93) have

discussed the theoretical aspects of electron transfer in isolated systems. Both clusters and super molecules of the form [DA] and [D-bridge/spacer-A] have been studied and are generally found to be quite similar.

For typical van der Waals clusters of aromatic molecules and nondonor and nonacceptor solvent molecules or partners, one observes sharp excitation and emission spectra and Franck-Condon profiles and dynamics near the origin ($S_1 \leftarrow S_0$) transition much like those observed for the bare chromophore species. The typical exciplex-ET cluster or super molecule shows sharp absorption; very broad, very redshifted emission, often in conjunction with some sharp emission; a temporal relation between these emissions such that the sharp emission decays as the broad emission rises; and an apparent activation energy associated with the broad emission that only arises at $0_0^0 + \Delta E$. The data often suggest that only certain conformers are active in the ET processes no matter what the activation energy or even if the ET state is directly accessed without apparent dynamics. The dynamical behavior accompanying time evolution of the local or van der Waals excited state to the electron transfer state can be associated with either a structural change through intermolecular cluster modes or the magnitude of an electron exchange matrix element for the electronic process.

Super molecules or bichromophoric molecules were studied by the Zewail group in the mid-1980s (94, 95) and, more recently, by Levy and colleagues (78–80) with both rigid and nonrigid spacer or bridge species. The acceptor anthracene is excited, and the donor moiety is a substituted aniline with a low IP. This system is classified as a reductive photoexcited quencher. In all instances a local excited state is first reached and a barrier to ET is found; further vibronic excitation allows the formation of the ET or CT state. Careful study of $(CH_2)_n$-spacer shows that conformers of $n = 2, 4$ molecules form exciplex and ET states, whereas conformers of $n = 1, 3$ do not interact strongly enough to lower the ET state below the van der Waals locally excited state. The interaction for anthracene and N-methyl-N-alkyl-*p*-methoxyaniline is so strong and the ET state is low enough in energy that the ground state of the bichromophoric system takes on some charge-transfer character. The system can then be classified as a charge-transfer complex.

An interesting twist on these systems arises for a positive donor (naphthalene) and a positive charge acceptor (benzene, indole, or biphenyl) (79). Naphthalene is ionized, and the $D_2 \leftarrow D_0$ transition of the ion is monitored for rigid spacer molecules. When the positive charge migrates to the acceptor, the $D_2 \leftarrow D_0$ spectrum vanishes. The CT state risetime is less than 2 ns (the experimental time resolution) when it is thermodynamically accessible.

Lim and coworkers (81–85) have systematically studied clusters of substituted naphthalenes and anthracenes with aliphatic amines and ethers, and aromatic ethers. They excited both the acceptor origins and various vibronic features to follow the local to ET excited-state evolution. The two surfaces and their crossings determine the efficiency of exciplex formation. The ET appearance scales with the donor IP: Only low IP donors form an exciplex or ET low-lying excited state for the clusters.

Tramer and colleagues (86, 87) have studied anthracene and perylene (acceptor) and substituted benzene (donor) clusters. The properties of these complexes depend on the isolated energies and mixings of their D^+A^- excited states, which should depend on the IP and EA correlation discussed previously. Depending on these parameters and interactions, either pure locally excited or ET-state behavior can be observed.

A first-order theoretical understanding of these phenomena was previously reviewed (77) and has been expanded upon more recently. Jortner et al (92, 93) have discussed the specific situation for solvent-free super- or bichromophoric molecules. Their approach takes the existing theories of ET, based on solution kinetics, and relates them to intramolecular radiationless transitions involving low-frequency motions of the supermolecule. The quasi-continuum of intramolecular vibrational states acts as the thermodynamic bath for the ET process. Solution ET is modeled to occur as the local excited-state and ET-state potential energy surfaces "cross"; however, the approach of Jortner et al models isolated supermolecule ET as occurring from the region of the initially excited local potential energy surface. The model becomes similar to that for weak electronic-vibrational coupling within the context of radiationless transition theory (57–59). In traditional electronic-state coupling (e.g. S_0-S_1, S_1-T_n) the matrix elements involve vibronic perturbations (e.g. $\partial V/\partial Q$) and/or spin coupling terms; however, for ET-local van der Waals excited-state coupling, the matrix elements involve electron exchange operators. Even in solution with a continuous bath of solvent states, these terms are still thought to dominate the ET processes. The details of this approach generate a rate constant based on Fermi's Golden Rule and a standard energy gap law. This general framework should also apply to clusters with the intermolecular van der Waals modes serving as the quasi-continuum for the heat bath and density of vibrational states.

Oxidative Electron Transfer $D^*A \rightarrow D^+A^-$

In this type of electron transfer, the donor is excited and the IP of the excited donor and the EA of the acceptor facilitate the reaction indicated above. Examples of this type of reaction are formed for tertiary cage

amines azabicyclooctanes ($C_7H_{13}N$-ABCO and $C_6H_{12}N_2$-DABCO) and hexamethylenetetramine ($C_6H_{12}N_4$-HMT) clustered with amines and ethers (96–98), and for systems like benzenes clustered with tetracyanoethylene (77).

The discussion below focuses on the behavior of the polycyclic tertiary amine systems. These latter systems are quite interesting because their first excited electronic state is a 3s Rydberg state. This identification is verified through cluster-shift and excited-state lifetime studies as a function of cluster structure. Because the Rydberg 3s excitation is somewhat localized, both lifetimes and shifts depend on the site on the amine (e.g. N atoms, ethylene bridges) to which an inert solvent is coordinated. The solvation effects are largest at the site that maintains the highest 3s electron density. In fact, the electron density of the Rydberg state can be probed and determined by the size of the excited-state shifts and lifetime changes as a function of cluster structure.

The typical value of a cluster shift for ABCO and DABCO with an inert solvent (e.g. rare gas, CH_4, N_2) is $\sim +200$ cm^{-1} per solvent molecule. The lifetime of the 3s state drops from ~ 2 μs to less than 1 μs upon cluster formation. The lifetime decrease is due to enhanced intersystem crossing through symmetry reduction and the external heavy-atom effect. The triplet state is identified by its long lifetime and increased ionization energy.

Caged amine compounds clustered with ethers and amines (with empty Rydberg orbitals at comparable energies) show much different static and dynamic behavior. First, the cluster spectroscopic shifts are large and negative (~ -500 cm^{-1}). Second, spectra tend to be broad, complex, or have large Franck-Condon displacements. Third, the lifetimes become nonexponential and are characterized by a short time constant (~ 0.1 μs) signal plus a long time constant (> 100 μs) signal at roughly 20 to 30% of the initial signal intensity. Fourth, ionization of this long-lived state takes more energy than either the initially accessed singlet or triplet Rydberg state ionization energies. The new state is assigned as an electron- or charge-transfer state that is accessed from the singlet Rydberg state even at the origin transition. Clearly with these long times for electron transfer, the transition from the locally excited state to the ET state must have a considerable energy barrier, possibly associated with a structural rearrangement of the cluster. The situation for HMT is quite similar, but the decay times are ~ 0.02 μs for the triplet and not measurable within the resolution of the experiment for the ET state. Because the HMT molecule has four nitrogen atoms and high symmetry, cluster perturbations have a large effect on the dynamics. The overall behavior though should be much like that depicted in Figure 1.

PROTON TRANSFER

Proton-transfer reactions have been studied in cluster environments since the mid-1980s; the early efforts were carried out by Leutwyler and coworkers (99–102), who did spectroscopic studies to show emission characteristics of the anion in the naphthol-ammonia system. The general reaction behaves in the following manner:

$$\begin{aligned} \text{naphthol}(NH_3)_n &\xrightarrow{h\nu} \text{naphthol}^*(NH_3)_n \\ &\rightarrow \text{naphthate}^{*-} \cdots H^+(NH_3)_n \\ &\rightarrow \text{naphthol}^- \cdots H^+(NH_3)_n + h\nu' \\ &\rightarrow \text{naphthol}(NH_3)_n. \end{aligned}$$

The two photons involved in this cycle (ν and ν') are absorption and emission processes, respectively, with the emission being far red of the absorption ($\sim 10^4$ cm^{-1}) and broad. This early work was carried out without the aid of a mass spectrometer, and these authors suggested that the reaction occurs only for $n \geqslant 4$. The reaction only takes place for two basic reasons: (*a*) The pk_a of naphthol changes by ~ 10 units ($\sim 10 \rightarrow \sim 0$) upon S_0 to S_1 excitation ($h\nu$) (103); and (*b*) the basicity of ammonia clusters is quite large (104) and, one would predict, based on thermodynamics, that excited-state proton transfer would occur for $n \sim 3$ or more.

These early studies also suggest that unlike what one would predict based on thermodynamics, no proton transfer occurs for naphthol$(H_2O)_n$ clusters, even for n approaching 100. More recent studies of naphthol-water cluster (105, 106) suggest that proton transfer occurs for 1-naphthol$(H_2O)_n$ at n close to 30 but not at all for 2-naphthol-water clusters. For these two cluster systems, proton transfer apparently depends on solvent relaxation, reorganization, and cluster temperature.

Two other contributions round out the early phases of cluster proton transfer studies: (*a*) Zewail and coworkers (107) measured a decay time for a naphthol$(NH_3)_3$ of ~ 60 ps, which they attributed to a proton transfer time; and (*b*) Kim et al (108) found that one isomer of naphthol$(NH_3)_3$ has an ionization energy equal to that of the $n = 4$ cluster and that this value is 2000 cm^{-1} below that for other $n = 3$, 2, 1 ammonia clusters. The conclusions here are that proton transfer occurs for naphthol$(NH_3)_n$, $n \geqslant 3$, and that for the $n = 3$ cluster, the transfer process is close to threshold and depends on the structural details of the cluster.

Kim et al's (108) explanation of these structure and solvent findings can be represented as follows. The interactions between naphthol and its solvent species (in this instance, NH_3 and H_2O) can take two forms:

hydrogen bonding to the OH napthol moiety and dispersion interaction with the napthol π-system. For NH_3 the two interactions are comparable (probably 1200 vs 800 cm^{-1}, respectively), whereas for H_2O, they are quite different (probably 1800 vs 800 cm^{-1}, respectively). Moreover, the NH_3-NH_3 interaction is modest ($\sim$1000 cm^{-1}), whereas the H_2O-H_2O interaction is large ($\sim$2000 cm^{-1}). These estimates generate naphthol-water clusters that look like a drop of water hydrogen bonded though the alcohol group to naphthol and a naphthol-ammonia cluster that has a much more distributed structure. In the latter case, both the proton and the anion can be solvated or stabilized, but in the former case, only the proton is solvated. Of course, these structural constraints can readily account for the different behavior of the two cluster systems, even when transfer is thermodynamically allowed for a cluster of particular value of n. In solution these structural differences are not possible due to entropy considerations, and both liquid systems undergo proton transfer. In fact, high resolution-rotational coherence spectra (109, 109a) of naphthol with various solvents, while not conclusive, tend to bear out these above qualitative ideas on cluster structure (PM Felker, private communication), as do potential energy calculations (108).

The time-resolved studies of Hineman et al (110) on the naphthol-ammonia system (ROH, NH_3 and ROD, ND_3) include systematic energy, isotope, and cluster-size dependence studies of the observed dynamics. This work demonstrates that the time-dependent signals observed from $n = 3$ and 4 clusters are due to proton transfer and that this transfer occurs through a barrier penetration or tunneling mechanism. Additionally, a second time constant (100 to 1000 ps) is observed that can be assigned to solvent relaxation about the new charge distribution in the cluster following the proton transfer event.

The proton transfer mechanism can be modeled by a very simple potential surface with nearly quantitative agreement between calculational and experimental trends. The model consists of the following factors: 1. There is a one-dimensional potential surface with a harmonic well for the O-H motion, an inverted parabola barrier in the O-H$\cdots$N reaction coordinate, and a continuum (free particle) constant potential at the $O^- \cdots H^+N$ side of the barrier (see Figure 2); 2. The reaction is exothermic, so the product ($O^- \cdots H^+N$) side of the well is lower in energy than the reactant ($OH \cdots N$) side of the well (see Figure 2); and 3. IVR is very rapid, much faster than proton transfer, so energy placed in naphthol vibrational modes quickly finds its way into the van der Waals space, where it is statistically distributed according to the overall cluster density of states. Given these constraints, assumptions, and the above model potential, several qualitative comments can be made about this approach to proton transfer in

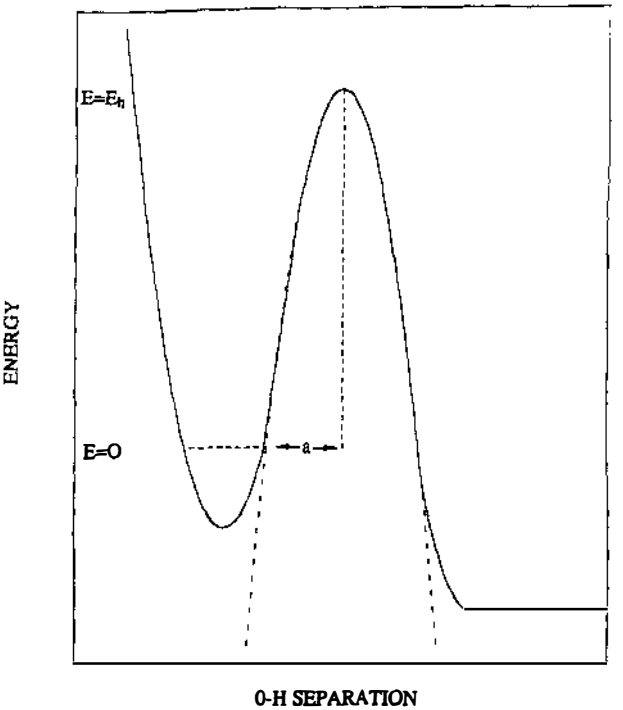

Figure 2 Schematic diagram of the potential model used for proton transfer rate calculations. The dashed line is the parabolic barrier, with parameters fit to origin $n = 3$ data. The solid curve is the barrier model, which includes a harmonic potential well with an OH vibrational energy of 3000 cm^{-1}. The well is centered at 1.0 Å. The other parameters for the model are $E_0 = 8700\ cm^{-1}$, $a_0 = 0.2$ Å, and the van der Waals stretch energy is 110 cm^{-1} for 1-naphthol$(NH_3)_3$. (See Reference 110 for more details.)

clusters. First, the clusters observed are at very low internal temperature (i.e. $T_{trans} \sim 0.1$ K, $T_{rot} \sim 3$ K, and $T_{vib} \sim 10$ K), so reorganization should be very slow, even following proton transfer with the added ΔH of reaction, which is probably greater than $10^3\ cm^{-1}$ at $n = 3$. In fact, following proton transfer, solvent reorganization is about a factor of 5 to 10 slower than the proton transfer event. Second, because the reaction is exothermic, the product well has a much higher density of states than the reactant well (at comparable energy), and thus, recrossing the barrier to regenerate reactant species is not very likely. Thus, the continuum product well assumption is probably not a major problem for the model; however, the model is readily augmented to include a product well and density of the states.

The rate of proton transfer is calculated by assuming a value (110 cm^{-1}) for the O···N van der Waals mode, calculating its excitation level and

using this motion to modulate the height and width of the barrier to proton transfer. In this way the tunneling rate constant ($k \propto 1/\tau$) depends on the vibrational energy of the cluster and the H-D isotope. The rate constant for each vibrational level of the O···N motion is calculated, and the total rate is given as the sum of the individual rates. Cluster geometry, Franck-Condon factors, and thermodynamics determine the relative rates for clusters of different size. The details of the calculation can be found in the original reference (110). Agreement between model calculations and experiments for the observed trends (the parameters, such as barrier height and width, are fit to a single measurement) is excellent.

Recently Zewail and coworkers (111) have presented a femtosecond study of naphthol-ammonia clusters in nearly the same manner as described above. The results are quite comparable to those of the previous time-resolved study and show quite clearly that no $\sim$100 fs–resolved dynamics occur in this proton transfer system. However, two aspects of the two time-resolved data sets (110, 111) appear different: (*a*) The H-D isotope effect on the proton transfer decay is much smaller in Reference 111 than that in Reference 110, and (*b*) the longtime solvent reorganization decays are much longer in Reference 111 than those in Reference 110. Although the decomposition of decays is not simple, these differences seem to be quite large (factors of 2 or 3) in many instances. Both studies do, however, agree as to the model and a semiquantitative understanding of the proton transfer process in naphthol-ammonia and -water clusters.

The other cluster system for which a number of proton transfer studies have been carried out is phenol-ammonia and -water system (112–116). The main results for this system are quite comparable to those discussed above. That is, phenol$(NH_3)_4$ undergoes excited-state proton transfer, and phenol$(NH_3)_3$ probably does not, and the times are quite comparable to those found for the naphthol system. The small water clusters of phenol do not experience proton transfer as is to be expected based on the naphthol-water system. Again, two decays are characterized as a function of excitation and ionization energies: H-D isotope effects and excess vibrational energy in the cluster. Nonetheless, a detailed proton transfer mechanism with a concomitant model potential surface cannot be characterized for this system because of extensive cluster ion fragmentation to generate $(NH_3)_xH^+$ clusters following ionization. Due to the Franck-Condon factors for ionization and the exothermicity of the reaction, the dynamics observed in a specific mass channel cannot be assigned to a specific parent cluster. The fragmentation pathways are found to be a function of excess energy in the cluster ion. Proton-transfer dynamics are found for all mass channels, $n = 1$ through 7, at ammonia concentration between 5 and 10% in the expansion (116). Because of these complications,

the phenol-ammonia cluster system cannot be employed as a test of the model for proton transfer proposed in earlier work on the naphthol-ammonia system. Nonetheless, the dynamics are shown to be related to proton transfer (H-D isotope affects) and tunneling; if the clusters could be ionized near threshold ($\sim$10,000 cm^{-1} lower in energy than is possible at present), fragmentation could be avoided, and a detailed model for the dynamics could be generated and verified. At present one can safely state that proton transfer does occur for phenol-ammonia systems and that the cluster ion fragments prior to detection owing to excess energy in the cluster ion.

REACTIVE INTERMEDIATE REACTIONS IN CLUSTERS-RADICALS, CARBENES, AND NITRENES

Gas-phase spectroscopic studies of reactive intermediates (e.g. radicals R·, carbenes R$\ddot{C}$R′, and nitrenes RN:) are numerous: Compendia of such studies abound. Gas-phase studies of solvated radicals have also been reviewed by Heaven (117), Lester and coworkers (118), and Miller and coworkers (119), although the frequency of these latter studies is dramatically reduced.

In the discussion for this section we consider systems that conform to our general theme and approach: Clusters of reactive intermediates are reviewed that have a high barrier to reaction on their ground state potential energy surface but not on their excited state surfaces. For such systems one has the possibility to access the reaction in or around the transition-state region and follow the reaction from reactant-like to product-like species. Because the present experimental approach relies on optical excitation, Franck-Condon factors control, to a large extent, the portion of the excited-state reactive potential energy surface accessed.

The results reviewed below are for the benzyl radical (BR)–ethylene system, which should be instructive as to the potential productivity of such studies. Spectra of reactive and reacting systems are typically quite broad, especially compared to comparable nonreactive systems. Moreover, the nature of the transition state (i.e. short-lived and not well-characterized) implies that sharp, recognizable, assignable spectroscopy features for reacting system spectra will be the exception rather than the rule (50, 51). Thus, theoretical calculations and modeling at the highest level tractable become a major component of the study of any reactive potential energy surface or transition state (50, 51).

Radical reactions of the above nature have been investigated both theoretically and experimentally for the BR-ethylene complex and theoretically for the methyl radical–ethylene complex on both ground- and

excited-state surfaces (120). Experiments begin with cluster formation, cooling, and subsequent laser excitation to the reactive excited state surface:

$$C_6H_5CH_2(C_2H_4)_1 \xrightarrow{h\nu} C_6H_5CH_2CH_2CH_2.$$

Reaction occurs for the first excited state but not the ground state, and the reaction appears to be adiabatic at least for the reaction coordinate displacement explored.

The results can be summarized as follows: 1. The binding energy for the $BR(C_2H_6)_1$ complex in D_0 and D_1 is $\sim 500\,cm^{-1}$; for $BR(C_2H_4)_1$ the binding energy is greater than 15,000 cm^{-1} (43 kcal mol^{-1}) in the D_1 state but only $\sim 600\,cm^{-1}$ for the D_0 state; 2. the spectrum for $BR(C_2H_6)_1$ is sharp, but for $BR(C_2H_4)_1$ is very broad, with only a few discernible features; 3. $BR(C_2H_4)_1$ ionization energy is $\sim 1000\,cm^{-1}$ less than that for $BR(C_2H_6)_1$, and the threshold is sharp for $BR(C_2H_6)_1$ but very broad for $BR(C_2H_4)_1$; 4. the D_1 lifetime is $\sim 1\,\mu s$ for $BR(C_2H_6)_1$ but $\sim 0.5\,\mu s$ for the high-energy $BR(C_2H_4)_1$ absorption; 5. deuteration has no effect on lifetime or nature of $BR(C_2H_4)_1$ spectrum; and 6. further solvation with another C_2H_4 has no obvious affect on the spectrum. Data and overall spectral features suggest an excited-state reaction has occurred for $BR + C_2H_4$ within the complex (half-collision environment). Calculations discussed below are consistent with this expectation.

Theoretical studies of this excited-state reaction are first explored for a simpler system, $CH_3(C_2H_4)_1$, in order to determine the appropriate level of calculation required to reproduce experimental results. The heat of reaction for this system in the ground state is known to be -25.5 kcal mol^{-1}, with an activation energy of 6.4 kcal mol^{-1} (121–123). In order to generate these results accurately, a calculation including a five-electron complete active self-consistent field (CASSCF) plus multireference configuration interaction (MRCI) (singles plus doubles) with a Davidson correction for higher-order electron correlation, and a double zeta valence (DZV) basis set must be employed. Within this framework the ground-state surface yields $\Delta E_{react} = -23$ kcal mol^{-1} and $\Delta E_{act} = 7.0$ kcal mol^{-1}. These results are very informative for the reaction coordinate in the ground state because they show the level of theory required to obtain agreement between theory and experiments. Excited-state results achieved at the same calculational level show that the reaction is exothermic (-30 kcal mol^{-1}) and has no activation energy and that the minimum on the excited-state surface falls at the same reaction coordinate value as the maximum on the ground-state surface. This latter result implies that the two potential surfaces undergo an anticrossing: Calculations make this clear because

root switching occurs near the crossing point. (See Figure 3 for a graphical representation of these results.)

These results instruct that in order to accurately calculate a bimolecular radical reaction on its ground- and excited-state potential energy surfaces, one must include extensive electron correlation through configuration interaction, the full virtual space for the CASSCF, a multireference (many Slater determinant configuration state functions) description of the state prior to configuration interaction, and as large a basis set as is acceptable for the calculational time and expense. These results are so encouraging that they are the main impetus for studying the CH_3-C_2H_4 reaction experimentally on its excited (both ethylene and methyl) state surfaces.

Based on this success, calculation for the $BR(C_2H_4)_1$ complex can be explored; however, one cannot at present expect to treat a 9- or 13-electron CASSCF/MRCI (S+D)/DZV system in a reasonable time frame. One must thus rely on a two-stage calibration in order to validate and correct the final nine-electron CASSCF calculation performed for the BR-ethylene excited-state reaction. First, a projected second-order Møller-Plesset (MP2) perturbation ground state calculation is employed for both CH_3-C_2H_4 and BR-C_2H_4 complexes. From these results good estimated values for the ground-state reaction heat and activation barrier are obtained.

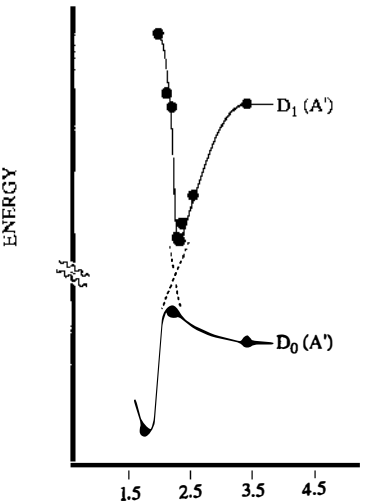

Figure 3 Calculated reaction coordinate between methyl radical and ethylene in the ground and first excited electronic states. (The ethylene species undergoes electronic excitation.) (See Reference 120 for more details.)

Second, in order to obtain values for the excited-state reaction, a nine-electron CASSCF calculation is performed on both ground- and excited-state surfaces. These ground-state values for ΔH and activation energy are corrected according to the calibrated MP2 ground-state values. These same corrections are employed to obtain estimates at the best level achievable (nine-electron CASSCF) for the excited-state reactions. These calculation show the same basic results for the BR-C_2H_4 and CH_3-C_2H_4 systems. The ground-state reaction for BR-C_2H_4 has a negative heat of reaction (-21 kcal mol^{-1}) and large activation energy (~ 11 kcal mol^{-1}). The excited state has a small barrier (<2 kcal mol^{-1}) and a -7 kcal mol^{-1} heat of reaction. In this instance a level anticrossing for the D_0 and D_1 surfaces is not apparent. Because one expects this procedure to yield high values of ΔH and the activation energy, the barrier on the excited-state surface is probably close to zero (see Figure 4).

Parallel studies of other systems are also in progress. Lester and co-workers (MI Lester, private communication) have made progress on

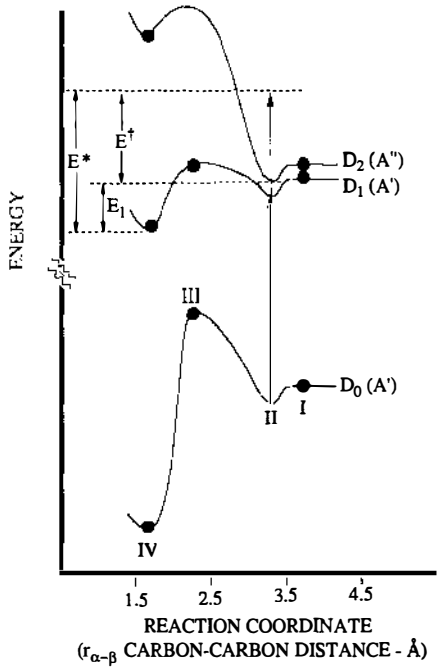

Figure 4 Calculated reaction coordinate between benzyl radical and ethylene in the ground and first two excited electronic states. (The benzyl radical species undergoes electronic excitation.) E_1 is the cluster binding energy. E^* is the vibrational energy in the cluster. $E\dagger$ is the excess energy in the cluster ($E^* - E_1$). (See Reference 120 for more details.)

$OH(N_2)_n$ and find some interesting line width results that depend on excited-state OH vibrations. Bernstein et al (J Bray, S Sun & ER Bernstein, unpublished data) are presently investigating CH_3-C_2H_4, OH-C_2H_4, and C_5H_5-C_2H_4 clusters for excited-state reaction dynamics.

Studies are also moving forward with regard to carbene and nitrene systems. The spectra of diphenyl carbene and difluorophenylnitrene have been investigated using laser photolysis (193, 266, 355, 532, and 1064 nm) of the respective diazo, ketene, and isocyanate compounds. These methods generate small fragments—such as C_2, NCO, CN—and encourage rearrangements (124) due to generation of highly excited electronic states of neutrals and ions (R Disselkamp, JL Yao, S Li & ER Bernstein, unpublished data). At present, efforts are underway to generate such species (JL Yao & ER Bernstein, unpublished results; GB Ellison & P Winter, unpublished results) through pyrolysis techniques (125–128).

CONCLUSIONS, PROSPECTS, DIRECTIONS

If there is one lesson to learn from the cluster chemistry reviewed in this article, it is that the use of van der Waals clusters to study chemical reaction potential energy surfaces is both important and successful. Clusters are an excellent experimental and theoretical construct through which to model the collision environment from a known initial set of conditions: structure, energy, energy distribution, and potential energy surface. How useful such studies will be over the next five to ten years will depend on the accessibility of the chosen systems to both theoretical and experimental approaches. Proton-transfer, electron transfer, and vibrational dynamics cases seem well explored and well understood. The study of reactive intermediate bimolecular reactions is just at its infancy, and one can anticipate significant activity in this area in the next few years.

ACKNOWLEDGMENTS

These studies have been supported by grants from NSF and ARO. I thank Drs. S. Sun and T. Selegue for helpful comments concerning this manuscript.

Literature Cited

1. Alfano JC, Martinez SJ, Levy DH. 1991. *J. Chem. Phys.* 94: 1673
2. Morter CL, Wu YR, Levy DH. 1991. *J. Chem. Phys.* 95: 1518
3. Weber PM, Buontempo JT, Novak F, Rice SA. 1988. *J. Chem. Phys.* 88: 1082
4. Weber PM, Rice SA. 1988. *J. Chem. Phys.* 88: 6107
5. Weber PM, Rice SA. 1988. *J. Chem. Phys.* 88: 6120
6. Weber PM, Rice SA. 1988. *J. Phys. Chem.* 92: 5470
7. Wittmeyer SA, Topp MR. 1993. *J. Phys. Chem.* 97: 8718
8. Ebata T, Ito M. 1992. *J. Phys. Chem.* 96: 3224
9. Smith PG, McDonald JD. 1992. *J. Chem. Phys.* 96: 7344
10. Hineman MF, Bernstein ER, Kelley DF. 1994. *J. Chem. Phys.* 101: 850
11. Connell LL, Ohline SM, Joireman PW, Corcoran TC, Felker PM. 1992. *J. Chem. Phys.* 96: 2585
12. Felker PM, Zewail AH. 1988. *Adv. Chem. Phys.* 70(1): 265
13. Burgi T, Droz T, Leutwyler S. 1994. *Chem. Phys. Lett.* 225: 351
14. Felker PM. 1992. *J. Phys. Chem.* 96: 7844
15. Henson BF, Venturo VA, Hartland GV, Felker PM. 1993. *J. Chem. Phys.* 98: 8361
16. Venturo VA, Felker PM. 1993. *J. Chem. Phys.* 99: 748
17. Venturo VA, Felker PM. 1993. *J. Phys. Chem.* 97: 4882
18. Pribble RN, Zwier TS. 1994. *Science* 265: 75
19. Bernstein ER, ed. 1990. *Atomic and Molecular Clusters.* Amsterdam: Elsevier
20. Bernstein ER, ed. 1995. *Chemical Reactions in Clusters.* New York: Oxford Univ. Press. In press
21. Bernstein ER. 1992. *J. Phys. Chem.* 96: 10105
22. Nowak R, Menapace JA, Bernstein ER. 1988. *J. Chem. Phys.* 89: 1309
23. Ohshima Y, Kohguchi H, Endo Y. 1991. *Chem. Phys. Lett.* 184: 21
24. Weber T, Smith AM, Riedle E, Neusser HJ, Schlag EW. 1990. *Chem. Phys. Lett.* 175: 79
25. Hobza P, Bludsky O, Selzle HL, Schlag EW. 1993. *J. Chem. Phys.* 98: 6223
26. Schauer M, Law K, Bernstein ER. 1985. *J. Chem. Phys.* 82: 726
27. Schauer M, Bernstein ER. 1985. *J. Chem. Phys.* 82: 3722
28. Wanna J, Bernstein ER. 1986. *J. Chem. Phys.* 84: 927
29. Warren JA, Bernstein ER. 1986. *J. Chem. Phys.* 85: 2365
30. Wanna J, Bernstein ER. 1986. *J. Chem. Phys.* 85: 3243
31. Wright TG, Spirko V, Hobza P. 1994. *J. Chem. Phys.* 100: 5403
32. Hobza P, Burgi R, Spirko V, Dopfer O, Muller-Dethlefs K, Schlag EW. 1994. *J. Chem. Phys.* 101: 990
33. Schutz M, Burgi T, Leutwyler S, Fischer T. 1993. *J. Chem. Phys.* 98: 3763
34. Schutz M, Burgi T, Leutwyler S. 1992. *J. Mol. Struct.* 276: 117
35. Feller D, Feyereisen MW. 1993. *J. Comput. Chem.* 14: 1027
36. Hobza P, Bludsky O, Selzle HL, Schlag EW. 1992. *J. Chem. Phys.* 97: 335
37. Hobza P, Selzle HL, Schlag EW. 1991. *J. Chem. Phys.* 95: 391
38. Hobza P, Selzle HL, Schlag EW. 1990. *J. Chem. Phys.* 93: 5893
39. Hobza P, Selzle HL, Schlag EW. 1992. *Czech. Chem. Commun.* 57: 1186
40. Ramackers JJF, Langelaar J, Rettschnick RPH. 1982. In *Picosecond Phenomena III*, ed. K Eisenthal, RM Hochstrasser, W Kaiser, A Laubereau, p. 264. Berlin: Springer-Verlag
41. Heppener M, Kunst AGM, Bebelaar D, Rettschnick RPH. 1985. *J. Chem. Phys.* 83: 5314
42. Heppener M, Rettschnick RPH. 1987. In *Structure and Dynamics of Weakly Bound Molecular Complexes*, ed. A Weber, p. 553. Dordtrecht: Reider
43. Ramackers JJF, Krijnen LB, Lips HJ, Langelaar J, Rettschnick RPH. 1983. *Laser Chem.* 2: 125
44. Ramackers JJF, van Dijk HK, Langelaar J, Rettschnick RPH. 1983. *Faraday Discuss. Chem. Soc.* 75: 183
45. Kelley DF, Bernstein ER. 1986. *J. Phys. Chem.* 90: 5164
46. Jouvet C, Solgadi B. 1995. See Ref. 20. In press
47. Wittig C, Zewail AH. 1995. See Ref. 20. In press
48. Wittig C, Sharpe S, Beaudet RA. 1988. *Acc. Chem. Res.* 21: 341
49. Shin SK, Chen Y, Nickolais S, Sharpe SW, Beaudet RA, Wittig C. 1991. *Adv. Photochem.* 16: 249
50. Neumark DM. 1993. *Acc. Chem. Res.* 26: 33
51. Davis MJ, Koizumi H, Schatz GC, Bradforth SE, Neumark DM. 1994. *J. Chem. Phys.* 101: 4708
52. Buck U. 1994. *J. Phys. Chem.* 98: 5190
53. Li S, Bernstein ER. 1992. *J. Chem. Phys.* 97: 792

54. Li S, Bernstein ER. 1992. *J. Chem. Phys.* 97: 804
55. Li S, Bernstein ER. 1992. *J. Chem. Phys.* 97: 7383
56. Shang QY, Moreno PO, Li S, Bernstein ER. 1993. *J. Chem. Phys.* 98: 1876
57. Schollkopf W, Toennies JP. 1994. *Science* 266: 1345
58. Avouris P, Gelbart WM, El-Sayed MA. 1977. *Chem. Rev.* 77: 793
59. Mukamel S. 1985. *J. Phys. Chem.* 89: 1077
60. Mukamel S, Jortner J. 1977. In *Excited States*, ed. EC Lim, p. 57. New York: Academic
61. Robinson DJ, Holbrook KA. 1972. *Unimolecular Reactions.* New York: Wiley
62. Steinfeld JI, Francisco JS, Hase WL. 1989. *Chemical Kinetics and Dynamics.* New York: Prentice Hall
63. Levine RD, Bernstein RB. 1987. *Molecular Reaction Dynamics and Chemical Reactivity.* Oxford: Oxford Univ. Press
64. Gilbert RG, Smith SC. 1990. *Theory of Unimolecular and Recombination Reaction.* Oxford: Blackwell
65. Levy DH. 1981. *Adv. Chem. Phys.* 47(1): 323
66. Beswick JA, Jortner J. 1981. *Adv. Chem. Phys.* 47(1): 363
67. Lin SH. 1980. *Radiationless Transitions.* New York: Academic
68. Nimlos MR, Young MA, Bernstein ER, Kelley DF. 1989. *J. Chem. Phys.* 91: 5268
69. Hineman M, Bernstein ER, Kelley DF. 1993. *J. Chem. Phys.* 98: 2516
70. Smith JM, Zhang X, Knee JL. 1993. *J. Chem. Phys.* 99: 2550
71. Outhouse EA, Bickel GA, Dremmer DR, Wallace SC. 1991. *J. Chem. Phys.* 95: 6261
72. Outhouse EA, Dremmer DR, Leach GW, Wallace SC. 1993. *J. Chem. Phys.* 99: 80
73. Kaziska AJ, Wittmeyer SA, Topp MR. 1991. *J. Phys. Chem.* 95: 3663
74. Kaziska AJ, Shchuka MI, Wittmeyer SA, Topp MR. 1991. *J. Phys. Chem.* 95: 5017
75. Bernstein ER. 1995. See Ref. 20. In press
76. Alberty RA, Silbey RJ. 1992. In *Physical Chemistry*, pp. 595–618. New York: Wiley
77. Haas Y, Anner O. 1988. In *Photoinduced Electron Transfer*, Part A, ed. M Fox, M Chanon, p. 305. Amsterdam: Elsevier
78. Shou H, Alfano JC, Van Dantzig NA, Levy DH. 1991. *J. Chem. Phys.* 95: 711
79. Chattoraj M, Laursen SL, Paulson B, Chung DD, Closs GL, Levy DH. 1992. *J. Phys. Chem.* 96: 8778
80. Van Dantzig NA, Shou H, Alfano JC, Yang NC, Levy DH. 1994. *J. Chem. Phys.* 100: 7068
81. Saigusa H, Lim EC. 1990. *J. Phys. Chem.* 94: 2631
82. Saigusa H, Lim EC. 1991. *J. Phys. Chem.* 95: 7580
83. Chakraborty T, Sou S, Lim EC. 1994. *J. Am. Chem. Soc.* 116: 10050
84. Chakraborty T, Lim EC. 1993. *J. Phys. Chem.* 97: 11151
85. Chakraborty T, Lim EC. 1993. *Chem. Phys. Lett.* 207: 99
86. Castella M, Millie P, Piuzzi F, Caillet J, Langlet J, et al. 1989. *J. Phys. Chem.* 93: 3949
87. Piuzzi F, Tramer A. 1990. *Chem. Phys. Lett.* 166: 503
88. Anner O, Haas Y. 1988. *J. Am. Chem. Soc.* 110: 1416
89. Zingher E, Haas Y. 1993. *Chem. Phys. Lett.* 202: 442
90. Wegewijs B, Hermant RM, Verhoeven JW, Kunst AGM, Rettschnick RPH. 1987. *Chem. Phys. Lett.* 140: 587
91. Wegewijs B, Ng AKF, Rettschnick RPH, Verhoeven JW. 1992. *Chem. Phys. Lett.* 200: 357
92. Jortner J, Bixon M, Heitele H, Michel-Beyerle ME. 1992. *Chem. Phys. Lett.* 197: 131
93. Jortner J, Bixon M, Wegewijs B, Verhoeven JW, Rettschnick RPH. 1993. *Chem. Phys. Lett.* 205: 451
94. Felker PM, Syage JA, Lambert WR, Zewail AH. 1982. *Chem. Phys. Lett.* 92: 1
95. Syage JA, Felker PM, Zewail AH. 1984. *J. Chem. Phys.* 81: 2233
96. Shang QY, Moreno PO, Bernstein ER. 1994. *J. Am. Chem. Soc.* 116: 302
97. Shang QY, Moreno PO, Bernstein ER. 1994. *J. Am. Chem. Soc.* 116: 311
98. Shang QY, Dion C, Bernstein ER. 1994. *J. Chem. Phys.* 101: 118
99. Chesnovsky O, Leutwyler S. 1985. *Chem. Phys. Lett.* 121: 1
100. Chesnovsky O, Leutwyler S. 1988. *J. Chem. Phys.* 88: 4127
101. Droz T, Knochenmuss R, Chesnovsky O, Leutwyler S. 1988. *Chem. Phys. Lett.* 144: 317
102. Droz T, Knochenmuss R, Leutwyler S. 1990. *J. Chem. Phys.* 93: 4320
103. Ireland JF, Wyatt PAH. 1976. *Adv. Phys. Org. Chem.* 12: 131
104. Kabarle P. 1977. *Annu. Rev. Phys. Chem.* 28: 445
105. Knochenmuss RD, Holton GR, Ray D. 1993. *Chem. Phys. Lett.* 215: 188

106. Knochenmuss RD, Smith DE. 1994. *J. Chem. Phys.* 101: 7327
107. Breen JJ, Peng LW, Willberg DM, Heikal A, Cong P, Zewail AH. 1990. *J. Chem. Phys.* 92: 805
108. Kim SK, Li S, Bernstein ER. 1991. *J. Chem. Phys.* 95: 3119
109. Connell LL. 1992. PhD thesis. Univ. Calif., Los Angeles
109a. Felken DM, Maxton PM, Schaeffer MW. 1959. *Chem. Rev.* 94: 1787–806
110. Hineman MF, Brucker GA, Kelley DF, Bernstein ER. 1992. *J. Chem. Phys.* 97: 3341
111. Kim SK, Wang JK, Zewail AH. 1994. *Chem. Phys. Lett.* 228: 369
112. Jouvet C, Lardeaux-Dedonder C, Richard-Viard M, Solgadi D, Tramer A. 1990. *J. Phys. Chem.* 94: 5041
113. Syage JA, Steadman J. 1991. *J. Chem. Phys.* 95: 2497
114. Steadman J, Syage JA. 1991. *J. Am. Chem. Soc.* 113: 6786
115. Steadman J, Syage JA. 1991. *J. Phys. Chem.* 95: 10326
116. Hineman MF, Kelley DF, Bernstein ER. 1993. *J. Chem. Phys.* 99: 4533
117. Heaven MC. 1992. *Annu. Rev. Phys. Chem.* 43: 283
118. Giancarlo LC, Randall RW, Choi SE, Lester MI. 1994. *J. Chem. Phys.* 101: 2814
119. Yang MC, Salzberg AP, Chang BC, Carter CC, Miller TA. 1993. *J. Chem. Phys.* 98: 4301
120. Disselkamp R, Bernstein ER. 1994. *J. Phys. Chem.* 98: 7260
121. Lide DR Jr, ed. 1985. *J. Phys. Chem. Ref. Data* 14: 1–1165
122. Castelhano AL, Griller D. 1982. *J. Am. Chem. Soc.* 104: 3655
123. Kerr JA. 1973. In *Free Radicals*, ed. J Kochi, 1: 1–36. New York: Wiley
124. Im HS, Bernstein ER. 1991. *J. Chem. Phys.* 95: 6326
125. Kohn DW, Clauberg H. 1992. *P. Chem. Rev. Sci. Inst.* 63: 4003
126. Kohn DW, Robles ESJ, Logan CF, Chen P. 1993. *J. Phys. Chem.* 97: 4936
127. Minsek DW, Chen P. 1993. *J. Phys. Chem.* 97: 13375
128. Rohrs HW, Wickham-Jones CT, Ellison GB, Berry D, Argrow BM. 1995. *Rev. Sci. Inst.* 66: 2430